AIP Physics of Plasmas

Estimation of pump-out and positive radial electric field created by electron cyclotron resonance heating in magnetic confinement devices

F. Castejón, S. Eguilior, I. Calvo, D. López-Bruna, and J. M. García-Regaña

Citation: Phys. Plasmas **15**, 012504 (2008); doi: 10.1063/1.2831063
View online: http://dx.doi.org/10.1063/1.2831063
View Table of Contents: http://pop.aip.org/resource/1/PHPAEN/v15/i1
Published by the American Institute of Physics.

Estimation of pump-out and positive radial electric field created by electron cyclotron resonance heating in magnetic confinement devices

F. Castejón, S. Eguilior, I. Calvo, D. López-Bruna, and J. M. García-Regaña
Laboratorio Nacional de Fusión, Asociación EURATOM-CIEMAT, 28040 Madrid, Spain

(Received 7 September 2007; accepted 12 December 2007; published online 29 January 2008)

A fast approximate technique for calculating the outward electron flux induced by electron cyclotron resonance heating in magnetic confinement devices with ripple is presented. A model based on Langevin equations that allows one to compute the microscopic flux into the loss cone in momentum space is used. The outward macroscopic electron flux is also obtained for given plasma profiles. This extra flux causes the onset of a positive ambipolar electric field whose time evolution is demonstrated to depend strongly on the poloidal damping for electrons. © *2008 American Institute of Physics*. [DOI: 10.1063/1.2831063]

I. INTRODUCTION AND MOTIVATION

Previous work shows the existence of an outward particle flux when electron cyclotron resonance heating (ECRH) is applied to plasmas confined in the TJ-II stellarator (see, e.g., Ref. 1). The flux was detected in those experiments by soft x rays and radiation measurements that presented the particularity of being toroidally asymmetric. Besides the direct radiation measurements, the ECRH-induced flux also manifests itself through enhanced hollowness in the density profiles, usually accompanied by more peaked electron temperatures.[2] This extra flux (often called *pump-out*) can be explained by an increase of the number of particles entering the loss cone in momentum space due to the enhancement of their perpendicular velocity component. When this happens, those particles are lost in a time scale much shorter than typical confinement times, hence increasing transiently the outward electron flux. Similar profiles have been observed in other stellarators (see Refs. 3 and 4) and tokamaks (see, e.g., Refs. 5 and 6), although the explanation does not need to be the same for both types of device. The enhanced electron flux creates an extra positive electric field (since ions are not directly affected by ECRH) and the ambipolarity condition is restored. The time scale for the creation of such electric field is correspondingly very short, and the collisional electron transport is reduced giving rise to a peaked electron temperature profile. This peaking cannot be explained only by the decrease in density but it is due to a real improvement of heat confinement. Such a confinement regime is called core electron root confinement in the frame of the Stellarator Profile Data Base collaboration.[7] A positive electric field may be created by any mechanism that enhances the electron radial flux, thus transiently unbalancing the ambipolarity condition, $\Gamma_e = Z\Gamma_i$, as it can happen with the appearance of a low order rational surface inside the plasma.[8]

The direct calculation of this flux implies solving the five-dimensional (5D) kinetic equation that takes into account collisions and resonant plasma-wave interaction as well as the spatial inhomogeneities. A different approach using adjoint techniques is adopted in Ref. 9. In the present work, we develop an alternative approximate method based on Langevin equations. The evolution of the electric field is also estimated, showing that the main observable time scale is given in terms of the electron poloidal damping in typical conditions of ECRH plasmas.

Our procedure involves the calculation of the electron flux in momentum space through the loss cone. This approach, when performed in a linear regime, is fast enough to be inserted in a transport code thus allowing to estimate the contribution of the pump-out to transport in the device. Another approach, which includes an approximated geometry and diffusion coefficient, has been recently developed in Ref. 10.

We define the loss cone as the region in momentum space where all particles pushed away from thermal equilibrium are lost quickly. In this work, such region is considered to be exactly a cone in the two-dimensional (2D) momentum space, although in complex devices such as stellarators, the loss cone is no longer a cone, but consists of several regions with different typical lifetimes. In addition, the electric field created by the pump-out will modify the particle orbits, and hence the loss cone. This effect will not be taken into account herein.

The remainder of this paper is organized as follows. Section II is devoted to summarize a previous work where Langevin equations for quasilinear wave-particle interaction are presented. Section III shows an approximate way to work out the flux driven by ECRH. The dynamics of the electric field created by this extra flux is presented in Sec. IV. Finally, conclusions come in Sec. V.

II. THE LANGEVIN EQUATIONS FOR QUASILINEAR WAVE-PARTICLE INTERACTION

The enhanced electron flux in space is due to the preferential pumping of particles perpendicularly to the magnetic field in the heating zone. Actually, ECRH can be understood as particle diffusion in momentum space along the vector

$$\mathbf{d} = Y_s \mathbf{e}_\perp + N_\parallel u_\perp \mathbf{e}_\parallel, \tag{1}$$

where $\parallel$ and $\perp$ stand, respectively, for the parallel and perpendicular directions to the static magnetic field, $\mathbf{u} = \mathbf{p}/mc$, $Y_s = s\omega_c/\omega$, $\omega_c = eB/m$ is the cyclotron frequency, s is a nonnegative integer number denoting the harmonic order, ω is the wave frequency, and m is the electron mass. In the following, we take $s=2$. For typical values of the heating parameters ($Y_s \sim 1$, $|N_\parallel|<1$, and $u_\perp \sim 10^{-2}$), $\mathbf{d}$ is approximately proportional to $\mathbf{e}_\perp$, which implies an increase in the rate of particles entering the loss cone and consequently an extra outward flux. Since the ion flux is not affected by ECRH, the ambipolarity condition requires the onset of a radial positive electric field able to stop the extra electron flux. This electric field is responsible for the reduction of collisional heat transport, giving rise to peaked temperature profiles. Whenever there is a change in ECRH deposition, a transient radial current must arise until the new equilibrium without unbalanced electron outflow is reached. As discussed in Sec. I, computing the extra outward flux is difficult since it implies solving a 5D kinetic equation [2D in momentum and three dimensions (3D) in position space].[9] Herein, we adopt a different approach based on Langevin equations for the microscopic dynamics of particles in phase space.[11] The results are equivalent to those obtained by using Fokker–Planck equations. The trajectory in momentum space, i.e., $\mathbf{u}(t)$, of a particle embedded in a wave field is the solution of the equations

$$\left(\frac{\mathrm{d}\mathbf{u}}{\mathrm{d}t}\right)_{\mathrm{ECRH}} = D_{\mathrm{cy}}^{1/2}\left[\left(\boldsymbol{\nabla} D_{\mathrm{cy}}^{1/2} + \frac{1}{|\mathbf{d}|}\boldsymbol{\xi}\right)\cdot \mathbf{d}\right]\mathbf{d}. \tag{2}$$

The first term on the right-hand side of Eq. (2) is the deterministic part of the Langevin equation and reads

$$\mathbf{F}(\mathbf{u},r) = \tfrac{1}{2}[\mathbf{d}\cdot\boldsymbol{\nabla} D_{\mathrm{cy}}(\mathbf{u},r)]\mathbf{d}, \tag{3}$$

where $\nabla_i = \partial/\partial u_i$, $i=\parallel,\perp$, and $D_{\mathrm{cy}}(\mathbf{u},r)$ is defined below. The stochastic part corresponds to the second term on the right-hand side of Eq. (2), for which we assume a statistically stationary Markovian process. Therefore, $\boldsymbol{\xi}$ is a two-dimensional random vector whose components take values in the interval $[-\frac{1}{2},\frac{1}{2}]$ and satisfy

$$\langle \xi_i(t)\rangle = 0, \quad \langle \xi_i(t)\xi_j(t+\tau)\rangle = \delta_{ij}\delta(\tau). \tag{4}$$

Here, δ_{ij} is the Kronecker delta, $\delta(\tau)$ is the Dirac delta distribution and, as usual, the brackets indicate an average over all possible stochastic realizations. The 2×2 matrix $D(\mathbf{u},r)$ is defined as

$$D(\mathbf{u},r)_{ij} = \sqrt{2D_{\mathrm{cy}}(\mathbf{u},r)}\frac{1}{|\mathbf{d}|}d_i d_j. \tag{5}$$

Finally, the coefficient $D_{\mathrm{cy}}(\mathbf{u},r)$ comes from the quasilinear diffusion in momentum space. It is proportional to the spectral density $\Phi(N_\parallel)$ and to the wave power density. Explicitly,

$$D_{\mathrm{cy}}(\mathbf{u},r) = \frac{w(r)}{|u_\parallel|\gamma}|\boldsymbol{\Pi}(\rho)\cdot\mathbf{e}|^2\Phi(N_{\parallel R}), \tag{6}$$

where $N_{\parallel R}=(\gamma - s\omega_c/\omega)/u_\parallel$ is the resonant refractive index, $\gamma=(1+\mathbf{u}^2)^{1/2}$ is the Lorentz relativistic factor, $\mathbf{e}$ is a unit vector proportional to the electric field of the wave, and

$$\boldsymbol{\Pi}(\rho) = (sJ_s(\rho)/\rho, -\mathrm{i}J'(\rho), \quad J_s(\rho)u_\parallel/u_\perp), \tag{7}$$

with J_s the Bessel functions of the first kind and $\rho = N_\perp u_\perp \omega_c/\omega$; i.e., the product of the Larmor radius times the perpendicular wave vector. The radial dependence in the above formulae comes through $w(r)$, which can be written in terms of the available power $P(r)$ and the average microwave beam radius b,

$$w(r) = \frac{P(r)e^2}{m^2c^3\omega\epsilon_0 b^2}. \tag{8}$$

The spectral density will be considered Gaussian in the reminder of the text, namely,

$$\Phi(N_\parallel) = \frac{1}{\sqrt{\alpha\pi}}e^{-1/\alpha(N_\parallel - N_{0\parallel})^2}, \tag{9}$$

where $N_{0\parallel}$ is the main refractive index of the microwave beam and we take a typical beam width $\sqrt{\alpha}=0.2$. The wave frequency ω is chosen to resonate with the electron cyclotron motion in the second harmonic ($s=2$) in the neighborhood of the magnetic axis $r=0$.

The following derivatives with respect to $\mathbf{u}$ are needed in order to compute the right-hand side of Eq. (2):[12]

$$\frac{\partial D_{\mathrm{cy}}}{\partial u_i} = \frac{w}{|u_\parallel|\gamma}\Bigg\{-\Phi(N_{\parallel R})\left[|\mathbf{e}\cdot\boldsymbol{\Pi}|^2\left(\frac{\delta_{i\parallel}}{u_\parallel}+\frac{u_i}{\gamma^2}\right) - \frac{\partial|\mathbf{e}\cdot\boldsymbol{\Pi}|^2}{\partial u_i}\right] + \Phi'(N_{\parallel R})|\mathbf{e}\cdot\boldsymbol{\Pi}|^2\frac{1}{u_\parallel}\left(-N_{\parallel R}\delta_{i\parallel}+\frac{u_i}{\gamma}\right)\Bigg\}, \tag{10}$$

$$\frac{\partial|\mathbf{e}\cdot\boldsymbol{\Pi}|^2}{\partial u_\parallel} = \frac{2J_s e_z}{u_\perp}\left(e_x\frac{sJ_s}{\rho} + e_z\frac{u_\parallel}{u_\perp}J_s\right), \tag{11}$$

$$\frac{\partial|\mathbf{e}\cdot\boldsymbol{\Pi}|^2}{\partial u_\perp} = 2\left(e_x\frac{sJ_s}{\rho}+e_z\frac{u_\parallel}{u_\perp}J_s\right)\left[\rho' e_x e_z\frac{u_\parallel}{u_\perp}J_s' \times\left(-\frac{sJ_s}{\rho^2}+\frac{sJ_s'}{\rho}\right) - e_z\frac{u_\parallel}{u_\perp^2}J_s\right] + 2e_y^2 J_s' J_s''\rho'. \tag{12}$$

We can include the effect of collisions in Eq. (2) in a simple approximate way,

$$\frac{\mathrm{d}\mathbf{u}}{\mathrm{d}t} = \left(\frac{\mathrm{d}\mathbf{u}}{\mathrm{d}t}\right)_{\mathrm{ECRH}} + \left(\frac{\mathrm{d}\mathbf{u}}{\mathrm{d}t}\right)_{\mathrm{coll}}, \tag{13}$$

by using the slowing down equations (see, e.g., Ref. 13),

$$\left(\frac{\mathrm{d}\mathbf{u}}{\mathrm{d}t}\right)_{\mathrm{coll}} = -\nu\mathbf{u}. \tag{14}$$

These equations, as written in Ref. 13, involve the modulus of the momentum and variations of the parallel momentum. The perpendicular collision frequency can be obtained by changing variables so that the slowing down parallel and perpendicular collision frequencies are given by

$$\nu = \begin{pmatrix} \nu_\perp & 0 \\ 0 & \nu_\parallel \end{pmatrix} = \begin{pmatrix} \nu_u\left[1-\left(\frac{u_\parallel}{u_\perp}\right)^2\left(\frac{1+Z}{\gamma}\right)\right] & 0 \\ 0 & \nu_u\left[1+\left(\frac{1+Z}{\gamma}\right)\right] \end{pmatrix}. \tag{15}$$

The slowing down momentum frequency is (in SI units)

$$\nu_u = \frac{\omega_p \Lambda}{2\pi n c^3} \frac{\gamma^2}{2u^3}. \tag{16}$$

Here, $\omega_p = \sqrt{ne^2/m\epsilon_0}$ is the plasma frequency and Λ is the Coulomb logarithm.

In order to include slowing down effects, we have chosen a simple collision operator. In the present case, we are ignoring the pitch angle scattering even though this may indeed affect the distribution function and hence the flux: The pitch angle scattering tends to flatten the distribution function, thus slightly reducing the flux into the loss cone.

The electron trajectories in momentum space may be computed by numerical integration of Eq. (13). Since the deterministic term is much larger than the stochastic one except in the vicinity of the resonance, we will neglect the stochastic part in this work. On the other hand, we will keep track of the effect of collisions, although we expect it to be small as far as microwave absorption happens at values of the electron velocity that are about twice the thermal velocity.

We choose a tokamak with ripple to perform the calculations instead of a (more complex) 3D stellarator because we are interested in studying the influence of heating on transport and not in the confinement properties of a given magnetic configuration. The plasma is a circular torus with major radius $R_0 = 1$ m and minor radius $a = 0.2$ m. The magnetic field on-axis is $B_0 = 1$ T, and we take a ripple that depends on the radial coordinate: $\epsilon = 0.08 + 0.27(r/a)^2$. The values of the latter are taken larger than typical values of a tokamak (actually similar to those of the TJ-II stellarator), so that its effect can be noticed easily. We consider a plasma equilibrium with the following profiles:

$$B_\phi(r,\theta) = \frac{B_0}{1 + \dfrac{r}{R_0}\cos\theta}, \tag{17}$$

$$n(r) = n_0[1 - (r/a)^4]^2 + 10^{-3} n_0, \tag{18}$$

$$T(r) = \frac{T_0}{2}\{\exp[-(r/0.2a)^2] + \exp[-(r/0.4a)^2]\}, \tag{19}$$

where $B_0 = 1$ T, $n_0 = 10^{19}$ m^{-3}, and $T_0 = 1$ keV. The absorbed power is computed by using a weakly relativistic dispersion relation.[14] The absorption coefficient, which is twice the imaginary part of the perpendicular component of the wave vector, is plotted in Fig. 1 for a Maxwellian distribution function. The transmitted power along the minor radius, which is proportional to the squared electric field and thus to the flux in momentum space, is plotted in Fig. 2. In these two figures, $r > 0$ ($r < 0$) corresponds to the low (high) field side. They show a strong spatial dependence of $P(r)$, especially at low $N_\parallel$, in the absorption area.

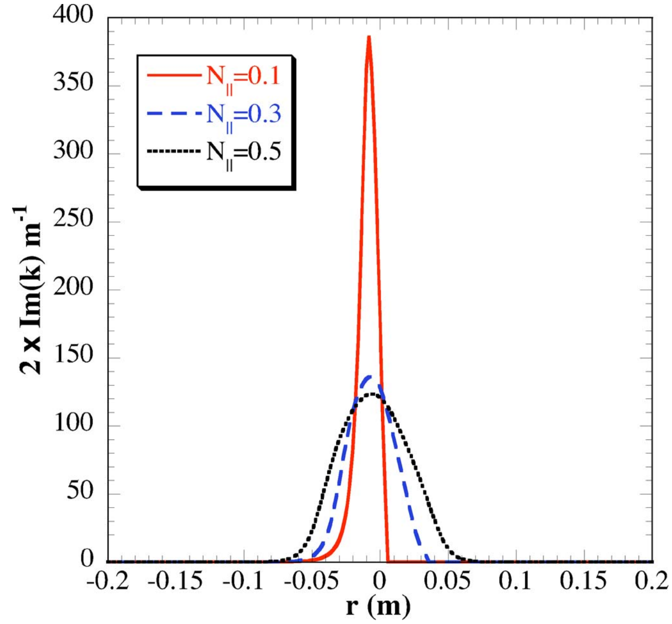

FIG. 1. (Color online) Absorption coefficient vs plasma radius for the profiles [Eqs. (17)–(19)] and three values of the parallel refraction index.

III. TRANSPORT ESTIMATES: LINEAR APPROXIMATION

The outward particle flux in space due to the pushing of electrons into the loss cone is related to the flux in momentum space through the loss cone surface. This pump-out flux is given (under certain approximations, see below) by

$$-\nabla \cdot \boldsymbol{\Gamma}^{\mathrm{ECRH}} = \left(\frac{\partial n}{\partial t}\right)_{\mathrm{ECRH}} = \int_\Sigma f(\mathbf{u}) \frac{\mathrm{d}\mathbf{u}}{\mathrm{d}t} \cdot \mathrm{d}\mathbf{S}, \tag{20}$$

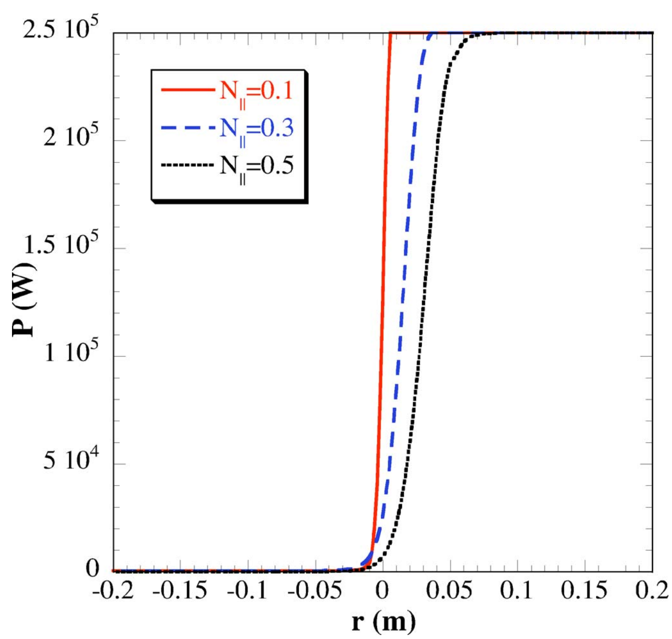

FIG. 2. (Color online) Transmitted power vs radius for the cases plotted in Fig. 1. The microwaves are launched from the low field side (positive r).

where Σ is the boundary of the loss cone in momentum space and $f(\mathbf{u})$ is the electron distribution function. We are assuming that all the electrons that enter the loss cone are lost immediately. In this expression it is necessary to know the distribution function and the exact structure of the loss cone in momentum space to estimate the flux of escaping particles. The knowledge of these two elements is equivalent to solving the problem, but we can introduce some approximations in order to do a quick calculation that allows us to extract the main properties of the ECRH-induced particle flux. Firstly, we assume that $f(\mathbf{u})$ is Maxwellian; i.e., the deformation of the distribution function due to transport and heating is small (we perform a linearization of the problem). Secondly, we consider that all particles entering the loss cone irreversibly escape from a magnetic surface that comprises the ECRH deposition zone. Finally, we assume that Σ is actually a cone characterized by a pitch angle θ of the electron trajectories. We also take the loss cone to be constant in time although, strictly, the distribution function will be modified by the interaction of the electrons with the waves and by the escaping particles; consequently the structure of the loss cone should be modified by the electric field. Under the above approximations, the flux can be written as

$$\begin{aligned}
-\boldsymbol{\nabla}\cdot\boldsymbol{\Gamma}^{\mathrm{ECRH}} &= \left(\frac{\partial n}{\partial t}\right)_{\mathrm{ECRH}} \\
&= 2\pi\int_{-\infty}^{+\infty} u_{\perp}\left(\frac{\mathbf{S}}{|\mathbf{S}|}\cdot\frac{\mathbf{d}}{|\mathbf{d}|}\right)\left|\frac{\mathrm{d}\mathbf{u}}{\mathrm{d}t}\right| f(\mathbf{u})\mathrm{d}u_{\parallel} \\
&= 2\pi\int_{0}^{+\infty} u_{\perp}\left(-\cos\theta\frac{\mathrm{d}u_{\perp}}{\mathrm{d}t}+\sin\theta\frac{\mathrm{d}u_{\parallel}}{\mathrm{d}t}\right) f(\mathbf{u})\mathrm{d}u_{\parallel} \\
&\quad + 2\pi\int_{-\infty}^{0} u_{\perp}\left(\cos\theta\frac{\mathrm{d}u_{\perp}}{\mathrm{d}t}+\sin\theta\frac{\mathrm{d}u_{\parallel}}{\mathrm{d}t}\right) f(\mathbf{u})\mathrm{d}u_{\parallel}.
\end{aligned} \tag{21}$$

Figures 3 and 4 show the structure of the flux through the loss cone in momentum space for $N_{\parallel}=0.1$ and $Y_s=1.01$, together with the loss cone and the resonance curve. Figure 3 gives the perpendicular component of the flux versus the parallel momentum, whereas the parallel component of the flux is shown in Fig. 4. For these values of $N_{\parallel}$ and of the magnetic field, the flux is well localized in momentum space. All the calculations are performed for X-mode at second harmonic.

Figure 5 shows the flux structure in momentum space for $N_{\parallel}=0.1$, at several radial positions and using the profiles introduced in the previous section. The pump-out in the center of the device is much larger due to the higher absorbed power density. The bulk of the pumped particles can have up to twice the thermal speed, which corresponds roughly to $|\mathbf{u}|=0.1$.

Given the temperature, the magnetic field, the power deposition profile, and making use of Eq. (21), the macroscopic perpendicular flux can be estimated, making the usual assumption that the plasma is homogeneous at every magnetic surface:

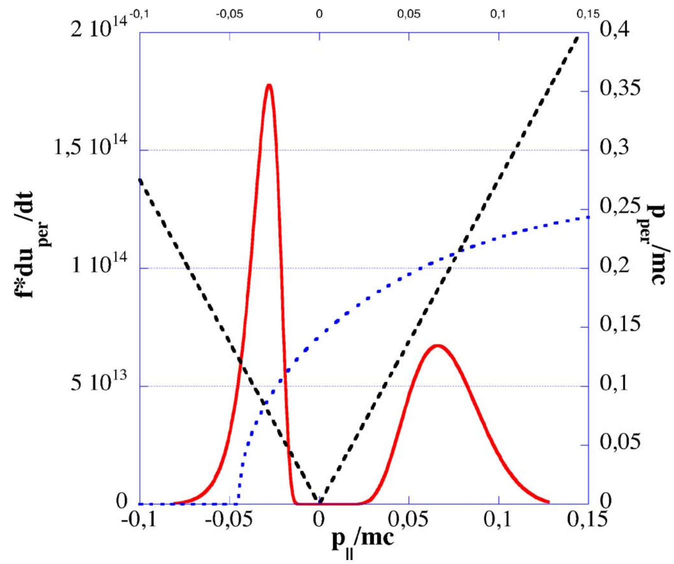

FIG. 3. (Color online) Structure of the perpendicular component of the flux in momentum space (solid line) for $N_{\parallel}=0.1$ and $Y_s=1.01$. The loss cone and the resonance condition (dotted lines) are also plotted.

$$\Gamma_r^{\mathrm{ECRH}}(r)=\frac{1}{r}\int_0^r \boldsymbol{\nabla}\cdot\boldsymbol{\Gamma}^{\mathrm{ECRH}} r'\mathrm{d}r'. \tag{22}$$

Figure 6 shows the divergence of the flux that gives the local contribution to the integrated flux, which is also plotted. The positive sign means outwardly directed flux. The most important contribution comes from the plasma core, where the absorbed power is maximum. The application of the ambipolarity condition implies that a radial positive electric field must be created to keep the plasma quasineutrality, as has been observed in many experiments (see, e.g., Ref. 15).

A procedure similar to the one presented in Eq. (21) can be used to estimate the Okhawa effect on electron cyclotron

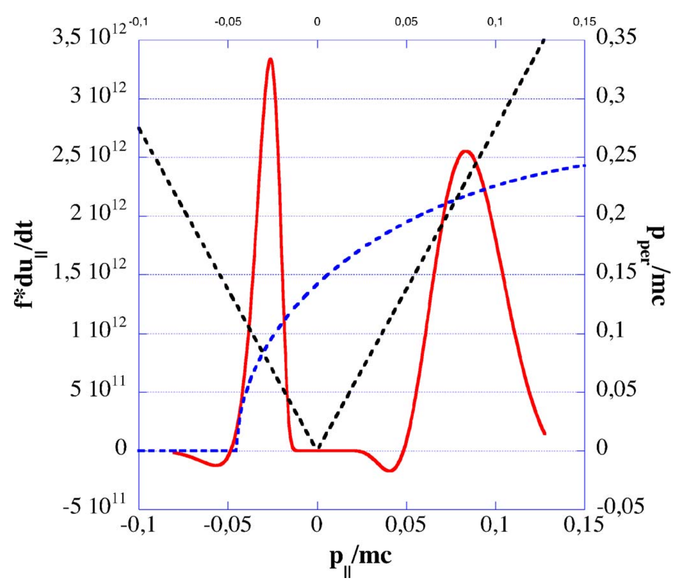

FIG. 4. (Color online) The same as Fig. 3 for the parallel component of the flux.

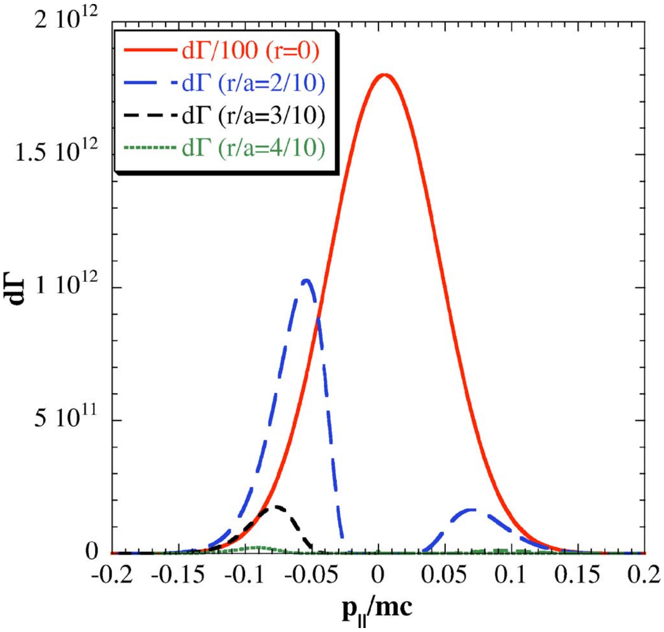

FIG. 5. (Color online) Structure of the flux in parallel momentum space, for $N_{\parallel}=0.1$, as given by Eq. (21), for the following radial positions: $|r/a|=0, 0.01, 0.02, 0.03$. The value at $r=0$ has been divided by 100 in order that the structure of the flux can be properly seen.

current drive. The asymmetric particle trapping rate in the positive and negative directions can cause a net plasma current. This asymmetry can be easily estimated using such an equation.

The energy spectrum of the particles that move outwards,

$$\Gamma(K) = \frac{1}{a}\int_0^a 2\pi u_{\perp}\left(\frac{\mathbf{S}}{|\mathbf{S}|}\cdot\frac{\mathbf{d}}{|\mathbf{d}|}\right)\left|\frac{\mathrm{d}\mathbf{u}}{\mathrm{d}t}\right| f(\mathbf{u}) r' \mathrm{d}r', \tag{23}$$

is plotted in Fig. 7, where we see that it presents a maximum that moves to larger energy values for increasing $N_{\parallel}$. The

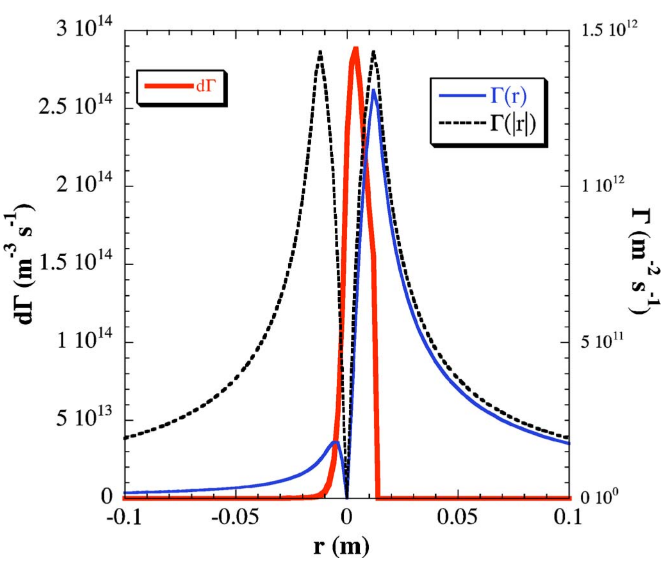

FIG. 6. (Color online) Divergence of the electron flux [Eq. (21)] vs radius (thick solid line). The flux [Eq. (22)] is also plotted (thin continuous line) together with the symmetrized flux (thin dashed line).

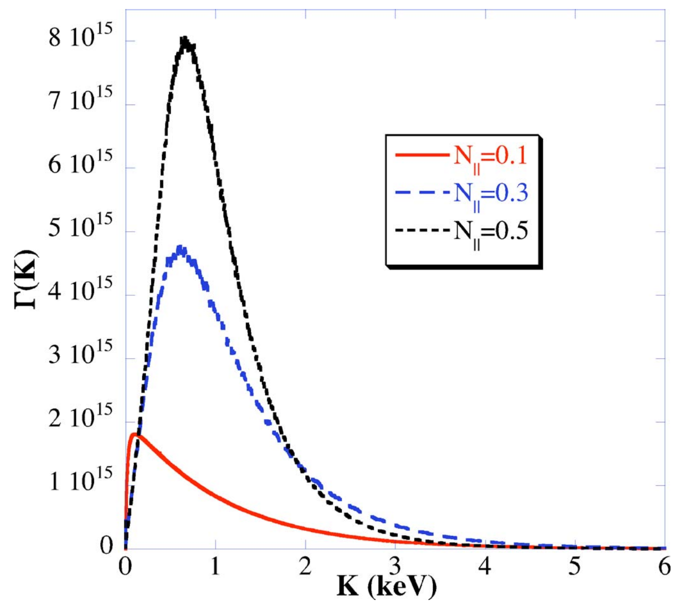

FIG. 7. (Color online) Particle flux of escaping particles as a function of energy.

particles that are expelled reach energies as large as 6 keV in this model, which means that superthermal electrons will escape to outer plasma positions and will be able to absorb power at those positions and to modify the measured x-ray spectrum. The faster particles will give an important contribution to the pump-out and will be the cause of the fast response, since the escape velocity is given by the combined curvature and ∇B drifts,

$$\mathbf{v}_{\nabla B} = \frac{m(v_{\parallel}^2 + 2v_{\perp}^2)}{2e}\frac{\mathbf{B}\times\nabla B}{B^3}. \tag{24}$$

It is worth discussing the appropriateness of neglecting the effect of the radial electric field through the $E\times B$ drift (that in general improves confinement by modifying the loss cone structure). For the plasma parameters considered herein, i.e., $E\sim 10^3$ V/m, in agreement with Ref. 16, and the $E\times B$ drift is smaller than $v_{\nabla B}$ for particles with $K\gtrsim 1$ keV, which indeed gives the most important contribution to the flux. Particles with $K\lesssim 1$ suffer the effect of collisions, with the consequent modification of the loss cone, which is suitably accounted for in our model. Our approximations affect particles with K in a narrow region centered at the value of the electrostatic potential (about 1 keV in our case), which collide at a moderate rate. Therefore, we are overestimating the flux slightly.

For the present plasma conditions, all the power absorption is localized in the vicinity of the resonance and little absorption happens at upshifted values of the magnetic field. The resonance condition implies that the energy of the particles ($mc^2\gamma$) is close to the thermal energy. In fact, the resonant energy in the quasiperpendicular propagation regime is given by $\gamma=B/B_0=R/R_0$. Therefore, if the absorption were small enough for making some power available at higher values of B, the resonance condition would allow higher energy particles.

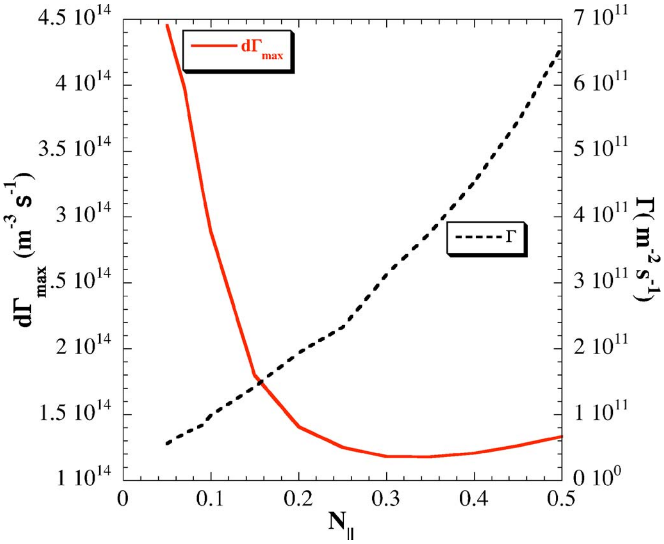

FIG. 8. (Color online) Maximum of the divergence of the flux [Eq. (21)] as a function of $N_{\parallel}$ (solid line) and total flux (dashed line) [Eq. (22)].

Figure 8 shows the maximum of the divergence of the flux and the flux itself as functions of $N_{\parallel}$. The maximum of the divergence is a decreasing function of $N_{\parallel}$. Hence, the pump-out is weaker because diffusion in momentum space tends to be directed parallel to the magnetic field. However, the total flux increases due to the fact that the power deposition profile becomes broader.

IV. TIME EVOLUTION OF THE ELECTRIC FIELD

The ambipolarity condition ensures that the perturbation of the radial electron flux by ECRH causes the onset of a positive radial electric field. This fact has been observed in modulation as well as in switch-on experiments in tokamaks and stellarators using a heavy ion beam probe (HIBP) (see, e.g., Refs. 16 and 17, respectively).

In this section we propose a simple set of first-order differential equations describing the behavior of the radial electric field at short time scales. Our simplifications are based on the conditions prevailing in the heating power deposition zone of typical TJ-II ECRH discharges: the ion flux remains roughly unperturbed and the density profile is almost flat or has a negligible gradient in comparison with that of the electron temperature.

If we start from the momentum balance equations (see, for instance, Refs. 18 and 19) and apply the former conditions, the equilibrium radial force balance imposes $\mathbf{E}\times\mathbf{B}$ rotation for the ion species and null rotation speed for the electrons, which can only be attained with the electrons being affected by a diamagnetic rotation exactly opposed to the $\mathbf{E}\times\mathbf{B}$ drift. For the conditions described above, this implies a radial electric field $E_r \approx -\nabla T_e/e$, as found in the experiments.[15] A model that reproduces these constraints is obtained considering that the ions are frozen, so that the dynamics at the time scales of interest is governed by the changes in the radial electron flux, Γ_r. In addition, we assume $E_\theta = E_\phi = 0$, $\Gamma_\phi = 0$, and $B_r, B_\theta \ll B_\phi$. In order to simplify the notation, $E \equiv E_r$ and $B \equiv B_\phi$. Our equations read

$$\partial_t E = \frac{e}{\epsilon_0 \epsilon_\perp}\Gamma_r, \tag{25a}$$

$$\partial_t \Gamma_r = -\frac{en}{m}E - \nu_r \Gamma_r + \frac{eB}{m}\Gamma_\theta - \frac{1}{m}\partial_r p, \tag{25b}$$

$$\partial_t \Gamma_\theta = -\frac{eB}{m}\Gamma_r - \nu_\theta \Gamma_\theta, \tag{25c}$$

where $\epsilon_\perp = (c/v_A)^2$, $v_A = B/\sqrt{\mu_0 n M}$ is the Alfvén velocity, and M is the proton mass. The large dielectric constant $\epsilon_\perp$ accounts for radial polarization current effects (see Ref. 20).

Clearly, the equilibrium solution is

$$E = -\frac{1}{en}\partial_r p, \quad \Gamma_r = \Gamma_\theta = 0, \tag{26}$$

and our aim is to find out how long it takes for the electric field to reach its equilibrium value. Defining

$$\mathbf{X} := \begin{pmatrix} E \\ \Gamma_r \\ \Gamma_\theta \end{pmatrix},$$

$$M := \begin{pmatrix} 0 & \frac{e}{\epsilon_0\epsilon_\perp} & 0 \\ -\frac{en}{m} & -\nu_r & \omega_c \\ 0 & -\omega_c & -\nu_\theta \end{pmatrix}, \tag{27}$$

$$\mathbf{Z} := \begin{pmatrix} 0 \\ -\frac{\partial_r p}{m} \\ 0 \end{pmatrix},$$

the set of equations (25) takes the form

$$\partial_t \mathbf{X} = M\mathbf{X} + \mathbf{Z}, \tag{28}$$

whose general solution, taking $t_0 = 0$, can be compactly written as

$$\mathbf{X}(t) = e^{Mt}\mathbf{X}(0) + \int_0^t e^{M(t-t')}\mathbf{Z}(t')\mathrm{d}t'. \tag{29}$$

The variations of $\mathbf{Z}(t)$ will correspond to transport time scales, much slower than those of interest in transient regimes of ECRH driven phenomena. Accounting for such slow variations cannot be done without (at least) one transport equation with E-dependent transport coefficients. We leave this for a future work and concentrate on the dynamics of E itself. Hence, the characteristic times of our problem are given by (the real part of) the eigenvalues of M. The characteristic equation of M is

$$P(\lambda) := \lambda^3 + (\nu_r + \nu_\theta)\lambda^2 + (\nu_r\nu_\theta + \Omega^2)\lambda + \nu_\theta \omega_p^2/\epsilon_\perp = 0, \tag{30}$$

where $\Omega = \sqrt{\omega_p^2/\epsilon_\perp + \omega_c^2}$.

Firstly, let us check that Eq. (25) is stable; i.e., that the solutions of the set of homogeneous linear equations

$$\partial_t \mathbf{X} = M\mathbf{X} \tag{31}$$

vanish when $t \to \infty$. Equivalently, we must show that if λ_i is a root of $P(\lambda)$, then $\mathrm{Re}(\lambda_i) < 0$. The real part of every root of $P(\lambda)$ is negative if and only if[21]

$$\nu_r + \nu_\theta > 0,$$

$$\nu_r \nu_\theta + \Omega^2 > 0,$$

$$\nu_\theta \omega_p^2 > 0,$$

$$(\nu_r + \nu_\theta)(\nu_r \nu_\theta + \Omega^2) > \nu_\theta \omega_p^2 / \epsilon_\perp,$$

which are obviously satisfied as long as $\nu_\theta \neq 0$.

$P(\lambda)$ is a real cubic polynomial; hence, it has at least a real root, which we denote by λ_1. Since the parameters ν_r and ν_θ are related, respectively, to radial and poloidal electron viscosities, $\nu_r, \nu_\theta \ll \Omega$. It is easy to see that in this situation

$$\lambda_1 \simeq -\frac{\nu_\theta}{\epsilon_\perp}\left(\frac{\omega_p}{\Omega}\right)^2. \tag{32}$$

Knowing λ_1, we can find the remaining two roots λ_2, λ_3 by factorization of $P(\lambda)$. It turns out that they are complex and consequently, $\lambda_3 = \lambda_2^*$. Explicitly,

$$\lambda_2 \simeq -\frac{1}{2}\left[\nu_r + \nu_\theta \left(\frac{\omega_c}{\Omega}\right)^2\right] + i\Omega. \tag{33}$$

We can get rid of the extremely fast, unobservable oscillations by averaging the solution $\mathbf{X}(t)$ over a few periods $2\pi/\Omega$. Denoting the averaged solution by $\langle \mathbf{X} \rangle(t)$,

$$\langle \mathbf{X} \rangle(t) = e^{\lambda_1 t}\langle \mathbf{X} \rangle(0) + \int_0^t e^{\lambda_1 (t-t')} \begin{pmatrix} -\frac{1}{en}\partial_r p \\ 0 \\ 0 \end{pmatrix} \mathrm{d}t', \tag{34}$$

whence we expect the observable time scales of E and Γ_θ to be the same and essentially governed by the electron poloidal damping ν_θ, which is given by the electron-ion collision frequency (note that we work with the *electron* radial force balance). Within our hypotheses, any initial condition $\Gamma_r \neq 0$ must decay to the equilibrium solution following the exponent given by Eq. (32). Therefore, if we start from an equilibrium field that satisfies the ambipolarity condition $\Gamma_e = Z\Gamma_i$, the final field will be the equilibrium one plus the extra field due to the increase in electron pressure gradient, provided that the ion flux remains unperturbed (or that its perturbation is negligible). Obviously, our variable for the radial flux must be interpreted in this context as $\Gamma_r = \Gamma_r^{\mathrm{ECRH}}$.

In a forthcoming work it will be shown that the response time of the electrostatic potential in the TJ-II flexible heliac is of the order of several milliseconds, which is in agreement with Eq. (32). In fact, for the present plasma conditions given by $T=1$ keV, $n=10^{19}$ m^{-3}, $B=1$ T, and $Z_{\mathrm{eff}}=2$, the collision frequency is $\nu_{ei} = 2Z_{\mathrm{eff}} \times 10^4$ s^{-1}, and $\epsilon_\perp = (c/v_{\mathrm{A}})^2 = 2.1 \times 10^2$. Therefore, the typical evolution time of the electric field is given by $\tau = -1/\lambda_1 \approx \nu_{ei}/\epsilon_\perp \approx 5$ ms. The equilibrium value of the electrostatic potential after a gyrotron has been switched on will be given by the value of electron temperature, provided that the density profile is almost flat, which happens in ECRH plasmas (see, e.g., Ref. 2), and the enhanced flux is zero once the steady state has been reached.

V. CONCLUSIONS

In this work, a linear estimation of the pump-out created by ECRH has been provided. The flux is obtained assuming that particles entering the loss cone are immediately lost and that the distribution function is Maxwellian; i.e., we deal with a plasma close to the equilibrium.

The divergence of the pump-out, or the rate of particle loss, is given by the integration of the electron flux through the loss cone in momentum space. Since no evolution of the distribution function is considered, the pump-out is proportional to the injected power. Despite the aforementioned approximation, this model allows the calculation of the ECRH-induced flux to be introduced, for instance, in a transport code. Moreover, it is suitable to explore the properties of the pump-out, such as the energy of the particles that escape from the plasma or the distribution of pump-out in momentum space.

Assuming that the ion flux is not modified by the ECRH, it is possible to estimate the electric field created by the heating, just applying the ambipolarity condition. The outward electron flux must be compensated by an ambipolar electric field whose evolution depends strongly on electron poloidal damping, which is given by collision frequency. The equilibrium value of the field after ECRH switch-on depends on how the heat transport is reduced by the electric field itself.

The particle trajectories in phase space could be obtained by combining the Langevin equations for heating with the guiding center equations. The latter are solved in Ref. 22 to calculate the ion kinetic transport in TJ-II. The guiding center equations together with the heating and the collision terms will give the modification of the particle and heat flux due to ECRH. The advantage of this heavy calculation is that it can be performed in a distributed way in many processors, which is suitable for the present clusters and computing grids.

ACKNOWLEDGMENTS

This work has been supported by the Spanish Ministerio de Ciencia y Tecnología under Project No. ENE2004-06957.

[1] M. A. Ochando and F. Medina, Plasma Phys. Controlled Fusion **45**, 221 (2003).
[2] F. Castejón, V. Tribaldos, I. García-Cortés, E. de la Luna, J. Herranz, I. Pastor, T. Estrada, and T.-I. Team, Nucl. Fusion **42**, 271 (2002).
[3] H. Maassberg, C. D. Beidler, U. Gasparino, M. Romé, K. S. Dyabilin, N. B. Marushchenko, and S. Murakami, Phys. Plasmas **7**, 295 (2000).
[4] A. Fujisawa, H. Iguchi, T. Minami, Y. Yoshimura, H. Sanuki, K. Itoh, S. Lee, K. Tanaka, M. Yokoyama, M. Kojima, S.-I. Itoh, S. Okamura, R. Akiyama, K. Ida, M. Isobe, S. Morita, S. Nishimura, M. Osakabe, A. Shimizu, C. Takahashi, K. Toi, Y. Hamada, K. Matsuoka, and M. Fujiwara, Phys. Rev. Lett. **82**, 2669 (1999).

[5] Z. A. Pietrzyk, C. Angioni, R. Behn, S. Coda, T. P. Goodman, M. A. Henderson, F. Hofmann, and O. Sauter, Phys. Rev. Lett. **86**, 1530 (2001).
[6] P. Buratti, E. Barbato, G. Bracco, S. Cirant, F. Crisanti, G. Granucci, A. A. Tuccillo, V. Zanza, M. Zerbini, L. Acitelli, F. Alladio, B. Angelini, M. L. Apicella, G. Apruzzese, L. Bertalot, A. Bertocchi, M. Borra, A. Bruschi, G. Buceti, A. Cardinali, C. Centioli, R. Cesario, C. Cianfarani, S. Ciattaglia, V. Cocilovo, R. De Angelis, F. De Marco, B. Esposito, D. Frigione, L. Gabellieri, G. Gatti, E. Giovannozzi, C. Gourlan, M. Grolli, A. Imparato, H. Kroegler, M. Leigheb, L. Lovisetto, G. Maddaluno, G. Maffia, M. Marinucci, G. Mazzitelli, P. Micozzi, F. Mirizzi, S. Nowak, F. P. Orsitto, D. Pacella, L. Panaccione, M. Panella, V. Pericoli Ridolfini, L. Pieroni, S. Podda, G. B. Righetti, F. Romanelli, F. Santini, M. Sassi, S. E. Segre, A. Simonetto, C. Sozzi, S. Sternini, O. Tudisco, V. Vitale, G. Vlad, and F. Zonca, Phys. Rev. Lett. **82**, 560 (1999).
[7] M. Yokoyama, H. Maassberg, C. D. Beidler, V. Tribaldos, K. Ida, T. Estrada, F. Castejon, A. Fujisawa, T. Minami, T. Shimozuma, Y. Takeiri, A. Dinklage, S. Murakami, and H. Yamada, Nucl. Fusion **47**, 1213 (2007).
[8] F. Castejón, A. Fujisawa, K. Ida, J. N. Talmadge, T. Estrada, D. López-Bruna, C. Hidalgo, L. Krupnik, and A. Melnikov, Plasma Phys. Controlled Fusion **47**, B53 (2005).
[9] S. Murakami, Nucl. Fusion **40**, 693 (2000).
[10] J.-C. Seol, C. C. Hegna, and J. D. Callen, Phys. Plasmas **14**, 082505 (2007).
[11] F. Castejón and S. Eguilior, Plasma Phys. Controlled Fusion **45**, 159 (2003).
[12] Several misprints that appeared in Ref. 11 have been corrected here.
[13] N. J. Fisch, Phys. Rev. A **24**, 3245 (1981).
[14] C. Alejaldre and F. Castejón, Phys. Fluids B **1**, 2201 (1989).
[15] F. Castejón, D. López-Bruna, T. Estrada, E. Ascasíbar, B. Zurro, and A. Baciero, Nucl. Fusion **44**, 593 (2004).
[16] A. V. Melnikov, L. G. Eliseev, S. V. Perfilov, A. A. Chmyga, A. D. Komarov, A. S. Kozachok, L. I. Krupnik, S. E. Lysenko, V. I. Tereshin, A. Alonso, J. L. de Pablos, A. Cappa, A. Fernández, C. Fuentes, C. Hidalgo, M. Liniers, M. A. Pedrosa, and TJ-II Team, Proceedings of 33rd EPS Conference on Plasma Physics, Rome, 19–23 June 2006, edited by F. De Marco and G. Vlad, ECA Vol. 30I (Associazione EURATOM-ENEA, Frascati, 2006), p. O-3.017 (CD-ROM).
[17] J. Sánchez, M. Acedo, A. Alonso, J. Alonso, P. Alvarez, F. de Aragón, E. Ascasíbar, A. Baciero, R. Balbín, L. Barrera, E. Blanco, J. Botija, B. Brañas, E. de la Cal, E. Calderón, I. Calvo, A. Cappa, J. A. Carmona, B. A. Carreras, R. Carrasco, F. Castejón, G. Catalán, A. A. Chmyga, N. B. Dreval, M. Chamorro, S. Eguilior, J. Encabo, L. Eliseev, T. Estrada, A. Fernández, R. Fernández, J. A. Ferreira, J. M. Fontdecaba, C. Fuentes, J. de la Gama, A. García, L. García, I. García-Cortés, J. M. García-Regaña, B. Gonçalves, J. Guasp, J. Herranz, A. Hidalgo, C. Hidalgo, R. Jiménez-Gómez, J. A. Jiménez, D. Jiménez, I. Kirpitchev, A. D. Komarov, A. S. Kozachok, L. Krupnik, F. Lapayese, M. Liniers, D. López-Bruna, A. López-Fraguas, J. López-Rázola, A. López-Sánchez, E. de la Luna, G. Marcon, F. Martín, L. Martínez-Fresno, K. J. McCarthy, F. Medina, M. Medrano, A. V. Melnikov, P. Méndez, E. Mirones, B. van Milligen, I. S. Nedzelskiy, M. Ochando, J. Olivares, R. Orozco, P. Ortiz, J. L. de Pablos, L. Pacios, I. Pastor, M. A. Pedrosa, A. de la Peña, A. Pereira, D. Pérez-Risco, A. Petrov, S. Petrov, A. Portas, D. Rapisarda, L. Ríos, C. Rodríguez, L. Rodríguez-Rodrigo, E. Rodríguez-Solano, J. Romero, A. Ros, A. Salas, E. Sánchez, M. Sánchez, E. Sánchez-Sarabia, X. Sarasola, K. Sarksian, C. Silva, S. Schchepetov, N. Skvortsova, A. Soleto, F. Tabarés, D. Tafalla, J. Tera, A. Tolkachev, V. Tribaldos, V. I. Vargas, J. Vega, G. Velasco, M. Weber, G. Wolfers, S. J. Zweben, and B. Zurro, Nucl. Fusion **47**, S677 (2007).
[18] K. C. Shaing, Phys. Fluids **29**, 2231 (1986).
[19] M. Coronado and J. N. Talmadge, Phys. Fluids B **5**, 1200 (1993).
[20] K. Itoh and S.-I. Itoh, Plasma Phys. Controlled Fusion **38**, 1 (1996).
[21] Let $p(x)=x^3+\alpha_2 x^2+\alpha_1 x+\alpha_0$ be a third-order polynomial with real coefficients and $\{x_i\}\subset\mathbb{C}$ the set of roots of $p(x)$. Then, $\mathrm{Re}(x_i)<0,\ \forall\ i$ if and only if $\alpha_2>0, \alpha_1>0, \alpha_0>0$ and $\alpha_2\alpha_1>\alpha_0$.
[22] F. Castejón, L. Fernández, J. Guasp, V. Martín-Mayor, A. Tarancón, and J. Velasco, Plasma Phys. Controlled Fusion **49**, 753 (2007).